Remote Sensing of Environment 258 (2021) 112358

Contents lists available at ScienceDirect

Remote Sensing of Environment

journal homepage: www.elsevier.com/locate/rse

Biophysical controls of increased tundra productivity in the western Canadian Arctic

Angel Chen [a], Trevor C. Lantz [a,*], Txomin Hermosilla [b], Michael A. Wulder [b]

[a] School of Environmental Studies, University of Victoria, Victoria, British Columbia, Canada
[b] Canadian Forest Service (Pacific Forestry Centre), Victoria, British Columbia, Canada

ARTICLE INFO

Keywords:
Landsat
Random Forests
Arctic tundra
Greening
EVI
Vegetation indices
Climate change

ABSTRACT

Rapid climate warming has widely been considered as the main driver of recent increases in Arctic tundra productivity. Field observations and remote sensing both show that tundra "greening" has been widespread, but heterogeneity in regional and landscape-scale trends suggest that additional controls are mediating the response of tundra vegetation to warming. In this study, we examined the relationship between changes in vegetation productivity in the western Canadian Arctic and biophysical variables by analyzing trends in the Enhanced Vegetation Index (EVI) obtained from nonparametric regression of annual Landsat surface reflectance composites. We used Random Forests classification and regression tree modelling to predict the trajectory and magnitude of greening from 1984 to 2016 and identify biophysical controls. More than two-thirds of our study area showed statistically significant increases in vegetation productivity, but observed changes were heterogeneous, occurring most rapidly within areas of the Southern Arctic that were: (1) dominated by dwarf and upright shrub cover types, (2) moderately sloping, and (3) located at lower elevation. These findings suggest that the response of tundra vegetation to warming is mediated by regional- and landscape-scale variation in microclimate, topography and soil moisture, and physiological differences among plant functional groups. Our work highlights the potential of the joint analysis of annual remotely sensed vegetation indices and broad-scale biophysical data to understand spatial variation in tundra vegetation change.

1. Introduction

Increases in temperature are predicted to profoundly alter the structure and function of global vegetation (Serreze et al., 2000; Stocker et al., 2013). In Arctic ecosystems, where temperatures are warming at more than twice the average global rate (Cowtan and Way, 2014; Pithan and Mauritsen, 2014), shifts in vegetation are already widespread (Bhatt et al., 2013; Jia et al., 2009). Analysis of satellite imagery from the last three decades across the Canadian Arctic has revealed rapid increases in vegetation productivity in the Yukon, Northwest Territories, Nunavut, and northern Quebec and Labrador (Ju and Masek, 2016).

Several lines of evidence indicate that changes in vegetation productivity have been driven primarily by increases in air temperature, a factor which significantly limits vegetation growth and reproduction at northern latitudes (Bunn et al., 2006; Myers-Smith et al., 2015; Ohse et al., 2012; Tape et al., 2012). Tundra warming experiments and fine-scale monitoring show that increasing temperatures can drive rapid expansion of deciduous shrubs (Jorgenson M. et al., 2018; Moffat et al., 2016; Travers-Smith and Lantz, 2020) and dwarf evergreen shrubs (Fraser et al., 2014; Rozema et al., 2009), but the magnitude of these changes is regionally variable (Elmendorf et al., 2015; Tape et al., 2012). Pronounced heterogeneity in vegetation productivity trends have also been observed at broad scales, with some tundra regions exhibiting rapid greening (Fraser et al., 2014; Jia et al., 2009), and others showing little to no change in productivity over the past few decades (Jorgenson J.C. et al., 2018; Tape et al., 2012). Research in some regions also indicates that trends in vegetation productivity are decreasing, or browning (Guay et al., 2014; Phoenix and Bjerke, 2016).

Heterogeneity of tundra productivity trends suggests that the effects of temperature are mediated by variation in local topography (Campbell et al., 2020; Ropars and Boudreau, 2012), surficial geology and geological history (Raynolds et al., 2006; Rickbeil et al., 2018), soil moisture (Cameron and Lantz, 2016; Campbell et al., 2020; Myers-Smith et al., 2015), and land cover (Bunn et al., 2006; Ju and Masek, 2016; Silapaswan et al., 2001). Research to determine the causes of this variability is critical because vegetation change affects ecological processes

* Corresponding author.
E-mail address: tlantz@uvic.ca (T.C. Lantz).

https://doi.org/10.1016/j.rse.2021.112358
Received 11 January 2021; Received in revised form 11 February 2021; Accepted 12 February 2021
Available online 7 March 2021

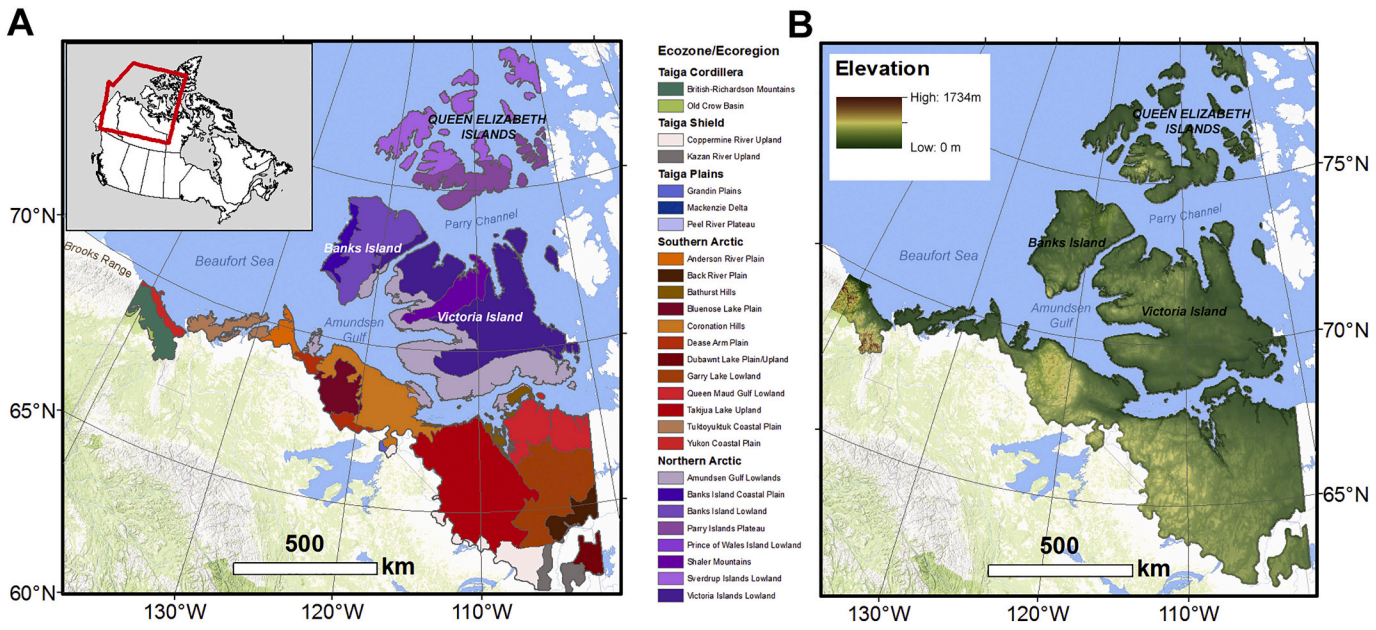

Fig. 1. (A) Map of the study region in the western Canadian Arctic overlaid with colours distinguishing ecoregions and ecozones located in this area. Inset map in upper left shows the extent of the 80-million hectare study area in north-western Canada. (B) Map of the study region overlaid with a Digital Elevation Model.

that strongly influence the climate system (Bhatt et al., 2017; Bunn et al., 2006; de Jong et al., 2013; Mcguire et al., 2009). Specifically, changes in the structure and function of tundra vegetation are expected to alter soil and permafrost conditions (Blok et al., 2010), hydrological processes (Drake et al., 2019), global carbon storage (Christiansen et al., 2018), and surface energy exchange (Blok et al., 2011).

In this study we used a time-series of Landsat imagery (Wulder et al., 2019) to analyze changes in the Enhanced Vegetation Index (EVI) from 1984 to 2016 and describe the spatial pattern and magnitude of vegetation change in the western Canadian Arctic. Our objective was to quantify changes in vegetation productivity and identify the biophysical variables that explain the spatial heterogeneity in observed trends. To accomplish this, we used Random Forests (RF) machine learning to model and evaluate the relationships between EVI trends and a suite of biophysical variables hypothesized to be influencing Arctic greening.

2. Methods

2.1. Study area

The study area for this project encompassed approximately 800,000 km^2 of Arctic tundra in the Yukon, Northwest Territories and Nunavut. (Fig. 1). Located between 63.5° N and 79.4° N and 141.0° W and 101.6° W, our study area consisted of the portion of western Canada defined as tundra by the circumpolar Arctic bioclimatic subzones map (Walker et al., 2005). This area spans the Taiga Cordillera, Taiga Plains, Taiga Shield, Northern Arctic, and Southern Arctic ecozones and 22 ecoregions that contain mosaics of graminoid tundra, prostrate-shrub tundra, erect shrub tundra, wetland vegetation, and sparsely vegetated barrens (Olthof et al., 2009; Walker et al., 2005). Mean July temperature across the study area ranges from 10 °C in the Taiga Cordillera to 4 °C in the Northern Arctic ecozone (Ecosystem Classification Group, 2013).

The terrain across our study area is highly variable. The western extent of our study area is located at the border of the Yukon and Alaska and is characterized by the low-lying Yukon Coastal Plain and glacial moraines that have been reworked by a range of periglacial processes, including hummock and thermokarst lake formation (Wolter et al., 2017). On the fringes of the Alaskan Brooks Range and south of the Beaufort Sea, this region extends inland westward through the Richardson Mountains, the Peel Plateau, and the Mackenzie Delta, towards the Arctic Archipelago. Moist and more nutrient-rich low-lying areas in this region are occupied by wet sedge, low shrub, and tall shrub communities, whereas hilltops, and alpine and exposed environments are characterized by dwarf shrub and herbaceous tundra (Smith et al., 2004; Ecosystem Classification Group, 2013). The islands of the Arctic Archipelago in the eastern extent of our study area are characterized by distinctive Northern and Southern Arctic ecoclimates. Northern Arctic regions like the Shaler Mountains, Banks Island Lowland and Parry Islands Plateau, are characterized by exposed bedrock, outwash deposits, glacial tills and plateaus. Upland vegetation in this region is mainly sparse and discontinuous, but in wet areas, a continuous cover of mosses, lichens, and low-growing forbs, sedges (including cottongrasses) can be found (Ecosystem Classification Group, 2013). Comparatively, vegetation in Southern Arctic regions like the Banks Island Coastal Plain and Amundsen Gulf Lowlands consists of near continuous dwarf shrub tundra which is often dominated by willows and sedges at wetter, warmer sites (Ecosystem Classification Group, 2013). The entire study area is located within the continuous permafrost zone, where a seasonally thawing active layer is found overlaying permafrost that ranges in depth from less than 100 m in areas with abundant water bodies to over 500 m in unglaciated regions (Burn and Kokelj, 2009). Cryosolic soils, characterized by the prevalence of permafrost, are the dominant soil order in this region (Tarnocai, 2004).

2.2. Enhanced Vegetation Index

To estimate shifts in vegetation productivity across our study area, we analyzed changes in the Enhanced Vegetation Index (EVI) calculated using Landsat imagery. EVI uses near infrared (NIR) and red wavelengths to relate biomass and photosynthetic activity, and employs blue wavelengths for aerosol correction to reduce the impact of spatially variable perturbations in the atmosphere (Huete et al., 2002).

$$EVI = 2.5 \times \frac{NIR - Red}{NIR + 6 \times Red - 7.5 \times Blue + 1}$$

Like the Normalized Difference Vegetation Index (NDVI), EVI has been used as a proxy for photosynthetic activity and productivity (Huete et al., 2002). In this analysis we chose EVI over other vegetation indices because it has greater sensitivity to soil moisture (Raynolds and Walker,

Table 1
Description of biophysical variables assessed as drivers of EVI trends.

Variable	Data set and source	Description	Resolution / scale
Land Cover	Northern Land Cover of Canada (Olthof et al., 2009)	Vegetation cover for Northern Canada	30 m [2]
Surficial Geology	Quaternary Geology of Canada and Greenland (Fulton, 1989)	Surficial geology classification	1: 5000000
Ecoregion	Terrestrial Ecoregions of Canada (Agriculture and Agri-Food Canada, 2013)	Subdivisions based on distinctive ecological features	1: 5000000
Elevation	Canada DEM (Natural Resources Canada, 2015)	Elevation above sea level	1: 250000
Aspect		Polar transformed aspect in eight cardinal directions	
Slope		Slope in degrees	
Topographic Solar Radiation Index		Continuous scale from 0 (coolest/wettest orientation) to 1 (hottest, driest orientation)	
Historical Summer Temperature	Climatic Research Unit Time Series (Harris et al., 2014)	Mean near surface temperature for July 1984	0.5°
Historical Winter Temperature		Mean near surface temperature for January 1984	
Precipitation	University of East Anglia Climatic Research Unit (Harris et al., 2014)	Mean precipitation for 1984	0.5°
Substrate Chemistry	Circumpolar Arctic Vegetation Map (Walker et al., 2005)	Classification of soil and bedrock chemistry	1 km^2
Lake Cover		Percent cover of lakes based on AVHRR data	

2016), subtle vegetation changes, canopy structure, plant phytomass and leaf area index (Kushida et al., 2015) and can diminish possible distortions present in NDVI values, which results from ground cover below a vegetation canopy (Xiao et al., 2005).

2.3. Landsat trend analysis

Changes in vegetation productivity were explored by calculating pixel-based trends in EVI using a time series of annual, gap-free, Landsat surface reflectance image composites from 1984 to 2016 produced using the Composite2Change (C2C) algorithm (Hermosilla et al., 2016). To do this, annual Best Available Pixel (BAP) Landsat composites were generated through pixel selection with user-determined scores for four criteria: (1) sensor type, (2) acquisition day of year (August 1st ± 30 days), (3) distance to clouds and cloud shadow, and (4) atmospheric opacity. Scores were summed and pixels with the highest score was assigned as the best pixel in the final raster composite. Data from outside of the collection date window were excluded and pixels where no observations were available (e.g., persistently cloudy locations) were labelled as data gaps (White et al., 2014). These BAP composites were further processed to remove unscreened noise (such as from thin clouds, haze or smoke) as well as non-permanent snow occurrences, and fill any remaining data gaps with proxy surface reflectance values using spectral trend information derived the temporal analysis of the time series (Hermosilla et al., 2015).

To calculate per-pixel trends in the EVI time series, we used the Theil Sen slope estimator (Sen, 1968). This is a non-parametric regression method for trend evaluation where the median slope of all pairwise

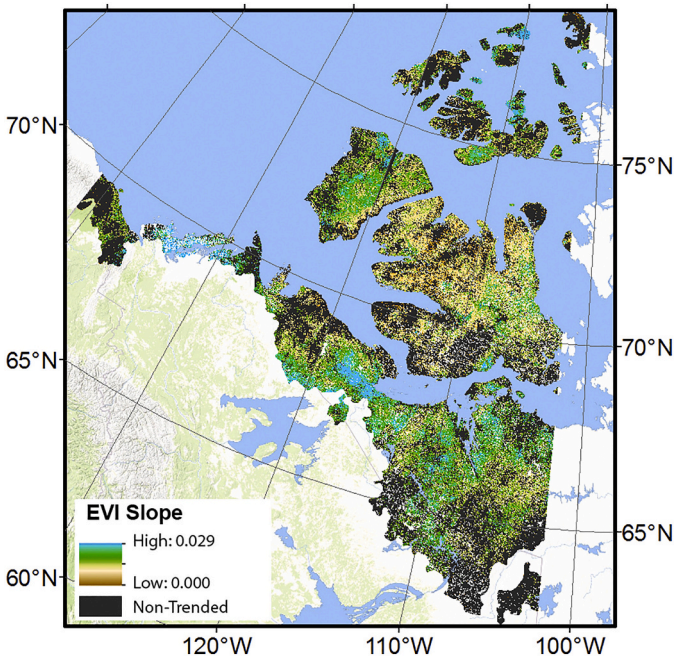

Fig. 2. Theil Sen slope of Enhanced Vegetation Index (EVI) trends for the study area from 1984 to 2016. Significantly greening trends ($p < 0.05$) determined using the Mann Kendall significance test are shown in colour and un-trended pixels are shown in black.

Table 2
Mean and median EVI trends by land cover type and the proportion of each cover type that experienced significant greening.

Land cover type	Median EVI Trend (year^{-1})	Mean EVI Trend (year^{-1})	Proportion Greening (%)
Tall Shrub	0.002155	0.002286	72.65
Low Shrub	0.001889	0.001990	**73.73**
Tussock Graminoid Tundra	0.001704	0.001774	**81.97**[a]
Graminoid/Dwarf Shrub Tundra	0.001533	0.001625	**73.68**
Wet Sedge	0.001339	0.001414	**78.49**[a]
Wetlands	0.001280	0.001452	**67.78**[a]
Bare Soil/Frost Boils	0.001091	0.001179	**79.11**[a]
Sparsely Vegetated Bedrock	0.001075	0.001434	**70.68**
Prostrate Dwarf-Shrub Tundra	0.001053	0.001219	**69.20**
Sparsely Vegetated Till	0.0007220	0.0008286	**67.24**
Barren	0.0005670	0.0007026	**58.68**[b]
Total study area	0.001105	0.001289	72.39
Non-significant area	0.0004340	0.0005304	27.61
Total greening study area	0.001401	0.001578	100

Bold text indicates where the difference between the proportion of greening for the land cover type is statistically different from zero based on alpha =0.05.
[a] Indicates where the proportion of greening for the land cover type is statistically greater than the proportion of greening for the study area based on an equivalence margin of Δ0.05.
[b] Indicates where observed greening is statistically less than the proportion of greening for the study area based on an equivalence margin of Δ0.05.

combinations is calculated. Repeated median estimates are more robust than ordinary least squares because they are less sensitive to outliers (Wilcox, 1998). All statistical analyses were performed in R (R Core Team, 2013) on Compute Canada's West Grid cloud-based high-performance computing infrastructure. We calculated the Theil Sen

Table 3
Proportion of each cover type that experienced significant greening in EVI trend delineated by ecozone.

Cover type	Northern Arctic (%)	Southern Arctic (%)	Taiga (%)
Tall Shrub	**73.08**	**76.85**	**57.21**
Low Shrub	**76.46**	**75.83**	**62.23**[a]
Tussock Graminoid Tundra	**64.37**[b]	**80.05**[a]	**66.53**[a]
Graminoid Dwarf Shrub Tundra	77.59	**74.76**	**50.00**[b]
Wet Sedge	**80.83**[b]	**78.38**	55.89
Wetlands	**68.34**[b]	**65.33**[b]	**48.25**[b]
Bare Soil/Frost Boils	**74.74**[b]	**69.62**[b]	56.25
Sparsely Vegetated Bedrock	**72.79**[b]	**67.97**[b]	**35.70**[b]
Prostrate Dwarf-Shrub Tundra	**79.75**[a]	**77.25**	**63.84**[a]
Sparsely Vegetated Till	**62.36**[b]	**60.32**[b]	**34.25**[b]
Barren	**63.09**[b]	**60.55**[b]	**44.22**[b]

Bold text indicates where the difference between the proportion of greening for the land cover type is statistically different from zero based on alpha = 0.05.

[a] Indicates where the proportion of greening for the land cover type is significantly greater than the proportion of greening for the study area based on an equivalence margin of 5%.

[b] Indicates where the proportion of greening for the land cover type is significantly less than the proportion of greening for the study area based on an equivalence margin of 5%.

estimator with the EcoGenetics package (Roser et al., 2020) and evaluated trends with the Kendall package (McLeod, 2011) by using the Mann-Kendall test for significance of monotonic trends in time series (Mann, 1945). Water masks generated using the Function of mask (Fmask) algorithm (Zhu and Woodcock, 2012) derived from Landsat Top of Atmosphere reflectance were used to remove water pixels and constrain the analysis to terrestrial pixels. Unlike areas of Scandinavia (Phoenix and Bjerke, 2016) and boreal Alaska (Verbyla, 2011) where significant decreases in productivity (browning) are spatially clustered and explicitly connected to specific regions and biophysical conditions, browning within our study area made up less than 1% of the total area and was not clustered. Since this small portion of browning pixels were not clustered, we masked out browning trends and focused on EVI trends classified as either: (1) significantly greening or (2) non-trended.

2.4. Modelling determinants of EVI greening

We used Random Forests (RF) (Breiman, 2001) regression and classification modelling to examine the relationships between tundra greening (slope of significant EVI trends) and 12 biophysical variables hypothesized to influence landscape scale vegetation dynamics (Table 1). RF models are a machine learning ensemble method based on classification and regression trees (CART). This approach uses sample-with-replacement to derive many sample subsets, or bootstrap samples. Different bootstrap samples are used to train each individual CART. Combining, or bootstrap aggregating (bagging) these CARTs creates the ensembled RF model. To calculate variance explained in our regression model we used out-of-bag (OOB) predictions to compute the percent of greening explained by data not used to train our model.

We ran both RF classification and RF regression models to separately evaluate the ability of biophysical factors to (1) distinguish areas with increasing EVI trends from non-trended pixels (classification), and (2) predict the marginal differences in the magnitude of greening in areas with positively trended pixels (regression). The 'caret' package (Kuhn, 2020) was used to downsample the majority class to address data imbalance in RF classification (Boulesteix et al., 2012). Regression and classification models were constructed using a random subset of 1% of

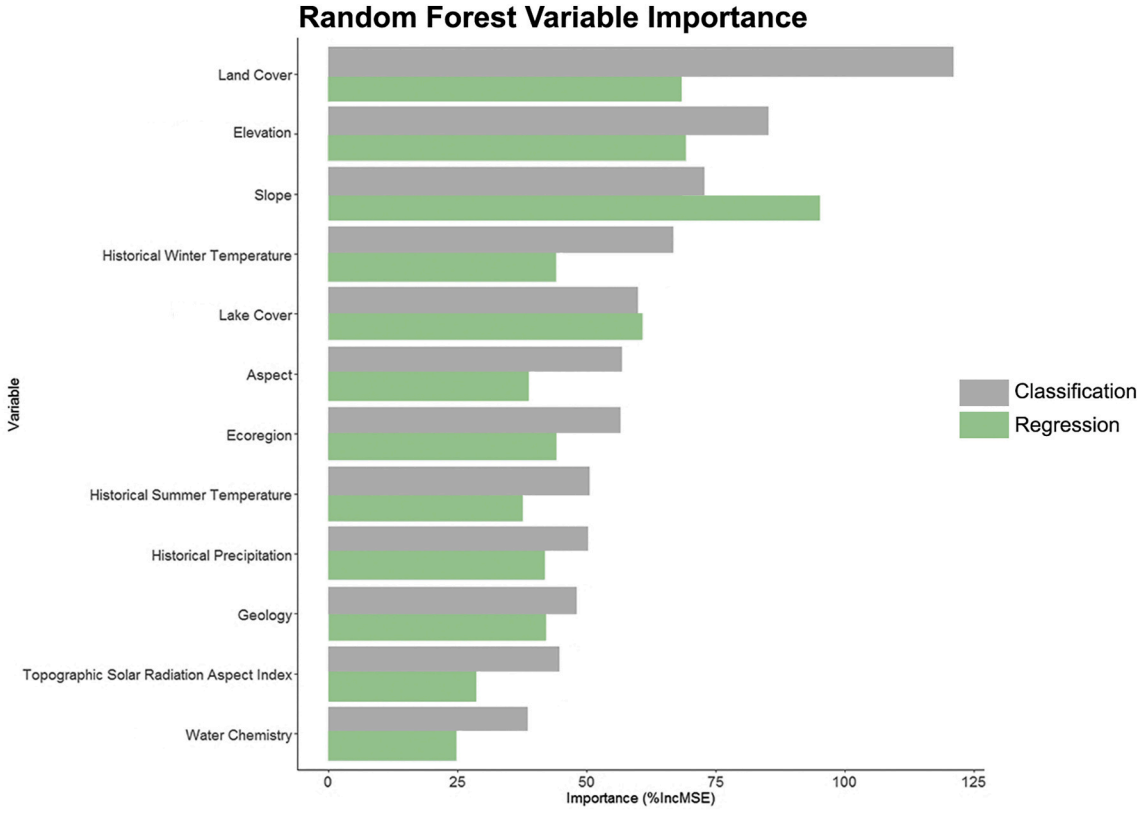

Fig. 3. Importance of biophysical variables from classification (green) and regression (gray) tree Random Forests models. Variables are arranged by classification variable importance, which is measured as the increase in mean square error (%Inc. MSE) when values of the predictor variable are randomly permuted and scaled by the normalized standard deviation of the differences. (For interpretation of the references to colour in this figure legend, the reader is referred to the web version of this article.)

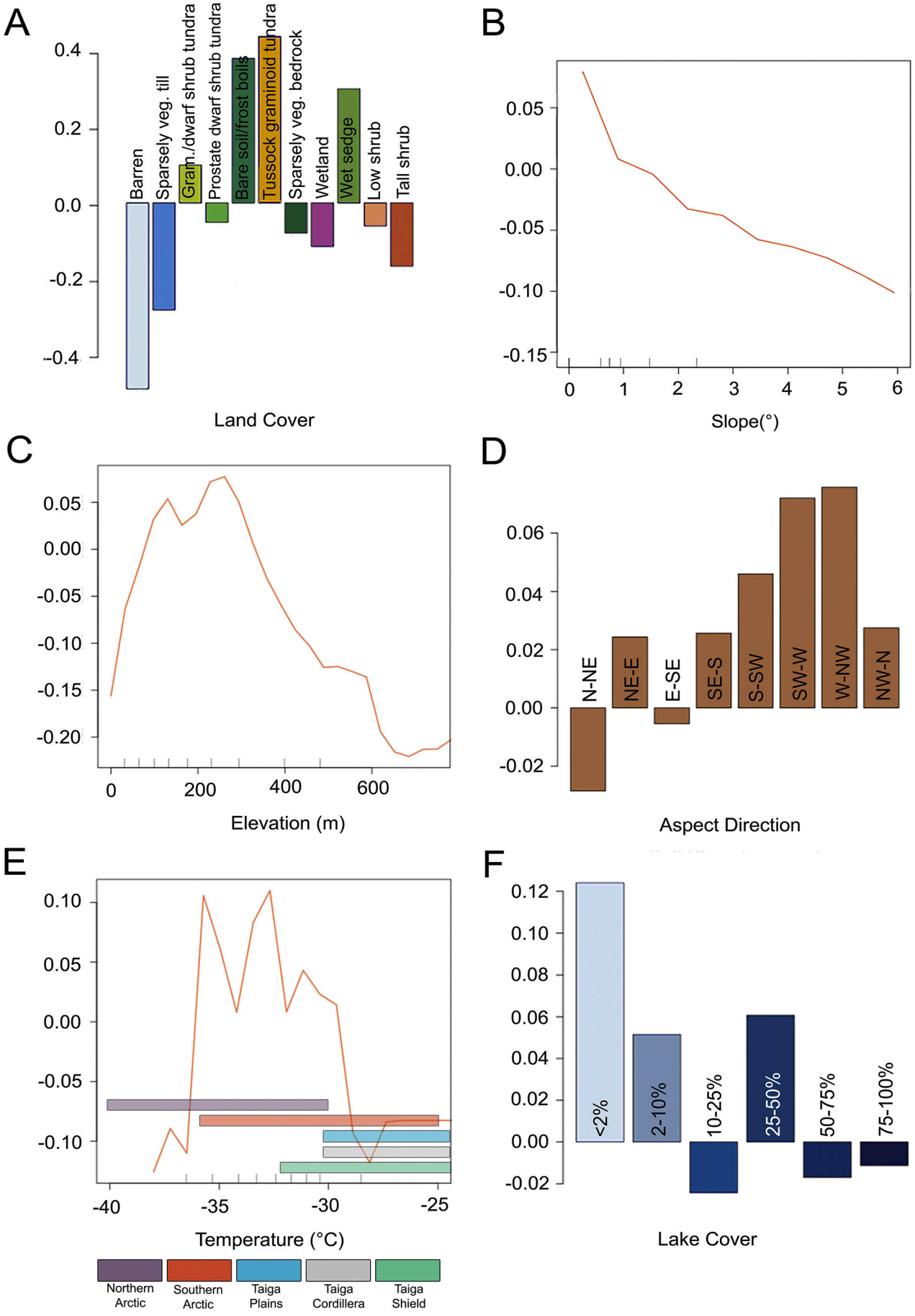

(caption on next page)

Fig. 4. Partial dependence plots for the six most important variables in the Random Forests classification model: (A) land cover (B) slope angle, (C) elevation, (D) aspect direction, (E) historical (1984) winter temperature with colored bars indicating temperature ranges in each ecozone, and (F) lake cover. Positive values on the y-axis indicate greater agreement between trees that a pixel is classified as greening at different values (x-axis) of a given explanatory variable, with the effect of other variables held constant (Friedman, 2001). Negative values indicate less agreement between trees that a level of the variable plotted was associated with greening.

the significantly greening pixels ($p<0.05$) in the study area and performed using the 'randomForest' package (Liaw and Wiener, 2018). We used the 'tidyverse' and 'dplyr' packages (Wickham et al., 2019, 2020) to preprocess, organize, and compile the random sample subset. To improve modelling efficiency, 'doParallel' and 'foreach' packages (Weston, 2019, 2020) were used to implement multiple cores for parallel processing.

Two one-sided tests for equivalence (Foody, 2009) were conducted using the 'TOSTER' package (Lakens, 2017) to test for equivalence (Tunes da Silva et al., 2009) between the proportion of greening of subgroups and the proportion of greening in our study area overall. These tests were based on the smallest effect size of interest ($d = 0.05$) (de Beurs et al., 2015). The two one-sided null hypotheses are 1) H_{01}: the difference between proportions is greater than or equal to the upper limit for equivalence ($\Delta \geq 0.05$), and 2) H_{02}: the difference between proportions is less than or equal to the lower limit for equivalence ($\Delta \leq -0.05$). If the difference between proportions was inside the equivalence bounds and the null hypotheses for both one-sided tests were rejected, then we conclude that the difference between proportions was smaller than the smallest effect size of interest and the proportions were deemed equivalent.

To evaluate and visually assess models, we used two analysis tools: (1) partial dependence plots and (2) mean decrease in model accuracy (%IncMSE). Partial dependence plots were used to visualize the marginal effects and patterns of the relationships between individual variables and modelled EVI trends when all other predictors are held constant. The y-axis of a partial dependence plot shows the mean of all model predictions for a given value of the predictor variable *(x)* (Jeong et al., 2016). We also used the variable importance function to rank the variables based on the percent increase in mean square error (%IncMSE) when values for a variable of interest are randomly permuted, effectively mimicking the absence of that variable from the model. The most important biophysical variables for explaining EVI trend have the greatest %IncMSE.

2.5. Biophysical variables datasets

Data for biophysical variables expected to influence trends in vegetation productivity were obtained from a range of sources (Table 1). Mean temperature and precipitation, which have been widely cited as driving forces of greening (Blok et al., 2011; Jia et al., 2009), were obtained from the University of East Anglia's Climatic Research Unit (CRU) Time Series 4.02 dataset (Harris et al., 2014; Harris et al., 2020). This gridded dataset covers all global land regions at a resolution of 0.5° from 1901 to 2017 and was derived using angular-distance weighted interpolation. We used data from July 1st and January 1st to assess both summer and winter historical temperatures from the beginning of the time series. Ecoregion data were acquired from the Terrestrial Ecoregions of Canada dataset published by Agriculture and Agri-Food Canada (2013). This dataset delineates ecoregions based on distinctive regional differences in environmental factors such as climate, physiography, vegetation, soil, water, and fauna. Data on lake cover and substrate chemistry were acquired from the Circumpolar Arctic Vegetation Mapping Project (Walker et al., 2005). Proximity to large water bodies and the effects on albedo have been suggested to contribute to vegetation greening along a forest-tundra gradient (Bonney et al., 2018) and hydrological changes associated with ice wedge degradation have altered surface water properties and vegetation across the western Arctic (Campbell et al., 2020; Liljedahl et al., 2016). Elevation data were obtained from the Canadian Digital Elevation Model (CDEM) (Natural Resources Canada, 2015). We used the 'spatialEco' package (Evans, 2020) to derive additional variables from the CDEM. These additional topographic variables included: slope, aspect, and the Roberts and Coopers (1989) topographic solar-radiation aspect index (TRASP), which transforms aspect to estimate relative solar radiation as continuous values from 0 to 1. Aerial photography and field research linking topographic position to increasing radial growth of *Betula glandulosa* demonstrates that variations in temperature and precipitation associated with terraces and hilltops can contribute to local heterogeneity of greening (Ropars et al., 2015). Data on surficial geology was taken from Fulton (1989) and aggregated into broad generic surficial units (ex. Lacustrine, Colluvial, Morainal, Fluvial). Spatial patterns of Arctic NDVI trends have been associated with landscape age and the effect of glacial history on vegetation type (Raynolds and Walker, 2009). Data on land cover were obtained from the Northern Land Cover of Canada dataset (Olthof et al., 2009). This land cover classification includes 15 classes north of the treeline (Timoney et al., 1992) and was derived from Landsat imagery at 30-m spatial resolution. Experimental warming studies have shown that warming can elicit different growth rates depending on cover type, where deciduous shrubs and graminoids have been observed to respond positively to warming while non-vascular plants such as mosses and lichens have responded negatively (Walker et al., 2006). All environmental datasets were reprojected to WGS84 reference ellipsoid and UTM coordinate system using nearest neighbour interpolation for categorical datasets and cubic convolution for continuous datasets and resampled to 30-m spatial resolution to match the resolution of the EVI data.

3. Results

3.1. EVI trends

Trends in the Enhanced Vegetation Index indicated widespread increases in vegetation productivity across the western Canadian Arctic (Fig. 2). Over 68% (540,000 km^2) of the study area experienced significant ($p<0.05$) greening (EVI slope > 0) between 1984 and 2016 and 31% of the study area (260,000 km^2) showed no significant trend in EVI over time. Land cover types where vegetation is less dense, such as sparsely vegetated till and barrens had comparatively lower EVI slopes than denser vegetation types (Table 2). The highest levels of greening were observed within the Southern Arctic zone in dense vegetation cover types, including tall shrub, low shrub, tussock graminoid tundra, and graminoid tundra, and dwarf shrub tundra (Table 3).

3.2. EVI classification model

The RF classification of significantly greening versus non-trended pixels had an overall OOB user's accuracy rate of 73.5% and a per-class accuracy of 76.4% for greening pixels and 70.4% for non-trended pixels. The average slope in non-trended pixels was 0.000005304 $year^{-1}$ and the average slope in greening pixels was 0.001578 $year^{-1}$ (Table 2). The six most important variables for determining if a pixel had a significant trend were: land cover, slope, elevation, lake cover, historical winter temperature, and geology (Fig. 3). These variables all increased model accuracy by more than 50%. Land cover was the most important biophysical predictor in the classification tree model and improved model accuracy by nearly twice as much as the next most important variable (Fig. 3). The partial dependence plot for land cover shows that bare soil, tussock graminoid tundra, and wet sedge were the cover classes with the highest probability of being classified as greening

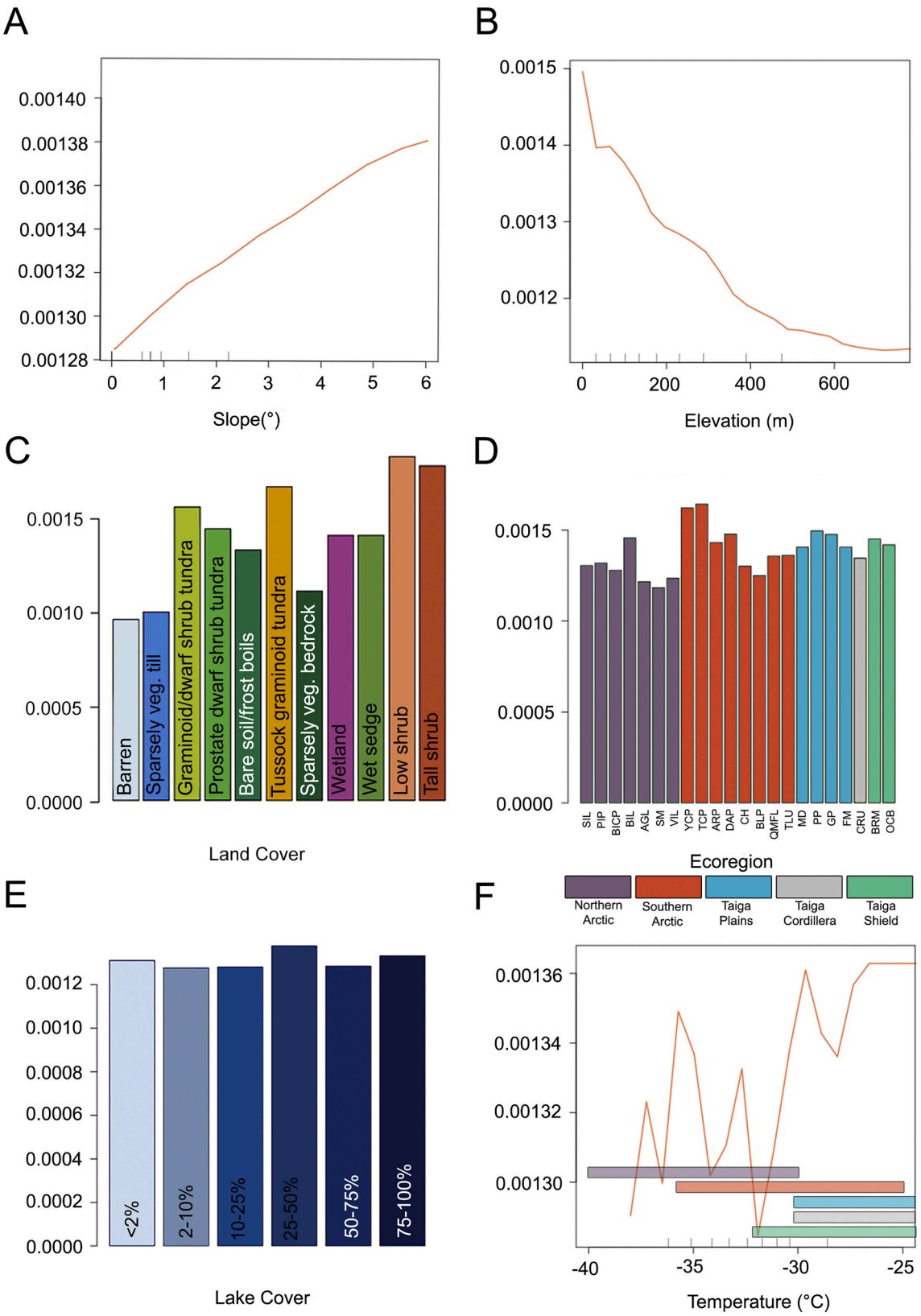

Fig. 5. Partial dependence plots for the six most important variables determined by Random Forests regression model: (A) slope angle, (B) elevation, (C) land cover, (D) ecoregion, (E) lake cover, and (F) historical (1984) winter temperature with colored bars indicating temperature ranges in each ecozone. The y-axis shows the average EVI trend slope predicted at different levels of a given explanatory variable, with the effect of other variables held constant (Friedman, 2001).

(Fig. 4A). Comparatively, barrens, sparsely vegetated till, and tall shrubs had a lower probability of containing greening pixels.

A suite of variables related to topography including elevation, slope, and aspect also had a large impact on the accuracy of the classification tree model (Fig. 3). Pixels at elevations between 100 and 350 m above sea level were more strongly associated with greening than low-elevation or montane areas (Fig. 4C). The partial dependence plot for slope indicated that flatter areas were more likely to be classified as greening (Fig. 4B) compared to sites with slopes greater than 5° (Fig. 4B). Glaciofluvial and glaciolacustrine sediments were more likely to be classified as greening than colluvium and rock. The overlap between the distribution of mountainous regions (Richardson Mountains, British Mountains, Shaler Mountains) in our study area and non-trended pixels is evident when comparing Figs. 1 and 2. Many parts of our study area are predominantly flat, but southern and western slopes were more likely to be classified as greening, while northern and eastern slopes were more likely to be classified as non-trended (Fig. 4D). A higher probability of greening was also associated with historical winter temperature between −36° and −28 °C and historical summer temperatures between 6 and 10 °C, which occur primarily in the lower Northern Arctic and upper Southern Arctic regions, such as Banks Island and Victoria Island, the Yukon Coastal Plain, Tuktoyaktuk Coastlands, and British-Richardson Mountains (Fig. 4E). The Southern Arctic experienced more rapid greening than the Northern Arctic and Taiga (Table 3). The partial dependence plot for lake cover indicates that the highest probability of greening occurred in areas with low (<10%) or moderate (25–50%) lake coverage (Fig. 4F).

3.3. EVI regression model

The biophysical variables used in RF regression model explained 48.4% of the variance in EVI slope, based on the out-of-bag (OOB) predictions. The six most important variables in the regression Random Forests model were slope, elevation, land cover, lake cover, ecoregion classification and historical winter temperature (Fig. 3). Topographic variables (slope, elevation) had the greatest impact on the accuracy of the regression model (Fig. 3). The partial dependence plot for slope shows that tundra greening was most rapid in areas with slopes between 3 and 6° (Fig. 5A). The partial dependence plot for elevation shows that the rate of greening was highest at low elevations and declined with increasing elevation (Fig. 5B). Elevation greater than ~ 500 m above sea level were uncommon across the study area and had a below average trend in EVI of 0.00100 year $^{-1}$.

The partial dependence plot for land cover indicates that the magnitude of greening was greatest in areas of denser and shrub-dominated vegetation, such as low shrub, tall shrub, graminoid dwarf shrub, and tussock graminoid tundra (Fig. 5C). Comparatively, the slowest greening trends were associated with largely non-vegetated land cover types, including barren and sparsely vegetated till (Fig. 5C). Glaciofluvial and morainal sediments experienced the fastest rates of greening while colluvium and marine sediments experienced the slowest rates. Rates of greening were similar across substrate chemistry classes.

The rate of greening also varied among ecoregions, with the greatest increases occurring in southwestern ecoregions including the Peel Plateau, Tuktoyaktuk Coastal Plain, Mackenzie Delta, and Yukon Coastal Plain. In these areas, median EVI trends were three to four times higher than the average trend across the entire study area (Fig. 5D, Table 2). The partial dependence plot for lake cover shows that the most rapid greening occurred in areas with moderate lake density, which are concentrated in the Mackenzie Delta, Tuktoyaktuk Coastal Plain, and Anderson River Plain. However, marginal differences among lake density classes were quite small (Fig. 5E). The relationship between winter temperature and EVI change showed considerable variation, but in general, winter temperatures below −30 °C were associated with smaller changes in vegetation productivity (Fig. 5F) and historical summer temperatures between 6 and 10 °C were associated with larger changes.

4. Discussion

Our observation that vegetation greening occurred across 68% of the study area and was common in all ecoregions suggests that this change was driven primarily by the rapid increases in temperature that have taken place across northwestern Canada (Meredith et al., 2019; Vincent et al., 2015). Increases in average annual air temperature of over 3°C since the mid 20th century (Overland and Wang, 2016; Vincent et al., 2015) and an extension of the growing season by nearly two weeks (Pedlar et al., 2015) parallel the conditions imposed by plot-scale tundra warming experiments, which have driven increases in stem biomass (Bret-Harte et al., 2001) net primary productivity (Wahren et al., 2005), and canopy height (Elmendorf et al., 2012a). The importance of climatic variables, including historical winter temperature and elevation, in our models of spatial variation in EVI trends also point to the importance of recent climate warming as a driver of change (Bunn et al., 2006; Jia et al., 2009). Partial dependence plots of historic winter temperatures show that greening was most likely to occur, and was most rapid, at temperatures typical of the Southern Arctic portion of our study area. This observation is similar to other recent studies showing that vegetation productivity has increased more rapidly in the Southern Arctic, and Taiga compared to the Northern Arctic (Berner et al., 2011; Bolton et al., 2018; Bonney et al., 2018; Reichle et al., 2018; Ropars and Boudreau, 2012; Sulla-Menashe et al., 2018). This is likely because vegetation productivity in the Northern Arctic is more severely limited by cold temperatures and a short growing season than the Southern Arctic (Svoboda and Henry, 1987; Raynolds et al., 2008; Epstein et al., 2008), where temperature limitation of growth and reproduction have been surpassed by recent warming (Elmendorf et al., 2012a; Lantz et al., 2013; Myers-Smith and Hik, 2018). This explanation is also consistent with our observation that sparsely vegetated cover types in the Northern Arctic (barren and till) had the lowest rates of EVI change and impacted the smallest area.

Recent studies in the Peel Plateau (Cameron and Lantz, 2016), the Tuktoyaktuk Coastlands (Fraser et al., 2014; Lantz et al., 2013; Travers-Smith and Lantz, 2020), and the Yukon Coastal Plain (Myers-Smith et al., 2011a, 2011b) also show evidence of widespread vegetation change that is consistent with our observations of accelerated Southern Arctic greening. In the southern extent of our study area greening was likely lower because the productivity of the Taiga forest that dominates these areas has been negatively impacted by increased drought and fire severity (Myers-Smith et al., 2015; Schut et al., 2015; Sulla-Menashe et al., 2018). It is also possible that the more complex vegetation structure found in proximity to the forest-tundra transition zone (treeline) complicates the use of Landsat imagery to detect tundra vegetation change (Boudreau and Villeneuve-Simard, 2012; McManus et al., 2012; Olthof and Fraser, 2007).

Although regional warming is likely the overarching driver of changes in productivity, our observation that slope, elevation, and aspect were among the most important variables in our classification and regression models suggests that soil moisture and microclimate can also mediate the impacts of warming on tundra vegetation productivity. The increased likelihood of greening on flat or gentle slopes (Fig. 4B), and the higher magnitude of greening on moderate slopes (Fig. 5A) indicates that moist to mesic conditions are most conducive to change. This is consistent with a recent study showing that increases in the productivity of upland tundra on Banks Island, NT were highest in flat areas accumulating moisture and nutrients from upslope (Campbell et al., 2020).

The higher probability of greening on south-southeasterly to west-northwesterly slopes also suggests that intermediate moisture conditions on moderately warm slopes have facilitated change (Dearborn and Danby, 2017). Partial dependence plots showing the effects of land cover and lake cover on EVI trends (Figs. 4A and 5C, E) also indicate that

greening was more widespread in mesic-moist land cover types (tussock tundra, shrub tundra, wet sedge), corroborating findings from other studies showing that increased productivity has been particularly rapid in riparian corridors, floodplains, along river valleys, and wetland-to-upland ecotones (Bonney et al., 2018; Loranty et al., 2016; Tape et al., 2012, Bunn et al., 2006; Ropars et al., 2015) (Bunn et al., 2006; Ropars et al., 2015). It is likely that areas with mesic conditions are experiencing higher than expected greening because carbon uptake and photosynthesis are higher at mesic sites compared to dry and wet sites (Kwon et al., 2006; Oberbauer et al., 2007). The effects of experimental warming on functional group abundance, community height, plant size, and leaf nitrogen content have also been shown to vary with temperature and soil moisture (Bjorkman et al., 2018; Elmendorf et al., 2012b).

Our analysis also suggests that spatial variation in tundra greening is driven by differences in the temperature sensitivity of some plant functional groups. Greening rates in productive cover types that are typically dominated by upright shrubs were more than 1.5 times higher than the average greening rate (Fig. 6; Table 2). Greening rates in sparsely vegetated cover types, characterized by low-growing herbs and prostrate shrubs, sedges, and mosses, were approximately half the average rate. These findings are also consistent with the results of experimental warming studies showing that shrub cover has increased in response to warming at warm, mesic sites (Elmendorf et al., 2012b). Plot-scale studies in the Southern Arctic also show that recent warming has increased the abundance of upright shrubs including willow (Myers-Smith et al., 2011a, 2011b), dwarf birch (Moffat et al., 2016; Tremblay et al., 2012), and alder (Frost et al., 2018; Lantz et al., 2013; Travers-Smith and Lantz, 2020). Areas dominated by upright shrubs are likely more responsive to warming-induced increases in resource availability because these woody plants can more efficiently allocate increased nitrogen and phosphorous to secondary growth and lateral expansion compared to other tundra species (Bret-Harte et al., 2001; Shaver et al., 2001). There are fewer plot-scale studies exploring the drivers of increased productivity in the Northern Arctic, but existing literature suggests that greening is linked with the accelerated growth of low-growing shrubs and herbs (Boulanger-Lapointe et al., 2014; Campbell et al., 2020; Edwards and Treitz, 2017; Weijers et al., 2017).

Findings from our classification and regression models were largely consistent with each other. However, unlike our regression model, which showed that shrub dominated cover types were greening the most rapidly, our classification model predicted that shrub dominated areas were more likely to not show trends in productivity over time. This is likely because shrub density can be patchy in these terrain types (Lantz et al., 2010; Moffat et al., 2016; Frost et al., 2018) and may exhibit more variable responses than other terrain types. Areas completely dominated by upright shrubs likely have less potential for increased productivity than patches occupied by a mix of shrubs and other tundra species. This is consistent with research in the Tuktoyaktuk Coastlands showing that shifts in the cover of plant functional groups were more variable in terrain dominated by upright shrubs compared to areas dominated by dwarf shrubs or graminoids (Moffat et al., 2016). At fine spatial scales, increases in shrub abundance have been greatest in areas that formerly had sparse cover of shrubs (Moffat et al., 2016; Cameron and Lantz, 2016).

Changes in tundra vegetation structure and composition are altering surface energy exchange (Chapin et al., 2005; Marsh et al., 2010), northern wildlife activity (Boelman et al., 2011; Van Hemert et al., 2015; Rickbeil et al., 2018), above and belowground carbon stocks (Schaefer et al., 2011; Schuur et al., 2015), and permafrost dynamics (Blok et al., 2010; Frost et al., 2018; Wilcox et al., 2019). Our study shows that greening is widespread across the western Canadian Arctic, but is more dominant and rapid in some areas. This indicates that the impacts of vegetation change on ecological processes will be heterogeneous and underscores the importance of fine-scale predictive models. Our analysis shows that changes have been most rapid in the Southern Arctic. Our work also highlights the potential of Random Forests modeling and other machine learning methods to contribute to the development of predictive models of tundra vegetation change (Bonney et al., 2018; Greaves et al., 2016). Inconsistency among greening trends derived from coarse-scale remote sensing platforms (Fisher and Mustard, 2007; Rocha et al., 2018) also points to the need for more regional- and landscape-scale analyses (Myers-Smith et al., 2020). Based on differences between plot-scale studies and remote sensing change detection (Goetz et al., 2019; Jorgenson J.C. et al., 2018; Myers-Smith et al., 2020), we suggest that future studies continue to evaluate change across multiple spatial scales and make use of the increasing availability and quality of high spatial and temporal resolution data sources, such as micro-satellites and remotely piloted aerial systems (Fraser et al., 2016; Liu and Treitz, 2018; Myers-Smith et al., 2019). Research examining physiological responses to changes in soil moisture, micronutrients and shifts in the below-ground community are also needed to understand the proximal controls to greening (Martin et al., 2017). With anticipated feedbacks between shifting tundra vegetation structure and the frequency of fire and thermokarst (Loranty et al., 2016; Swanson, 2017; Tsuyuzaki et al., 2017), additional research will also be required to understand how shifting disturbance regimes will shape vegetation trajectories. More frequent and extreme weather events (Bret-Harte et al., 2013; Hansen et al., 2014; Vermaire et al., 2013) that alter growing conditions are also likely to influence how tundra landscapes respond to ongoing climate change (Lantz et al., 2015).

5. Conclusions

Our analysis of trends in the Enhanced Vegetation Index shows that the tundra ecosystems of the western Canadian Arctic have undergone significant increases in productivity since 1984. The widespread nature of this greening, its association with historical temperature variation, and evidence from plot-scale warming experiments and observational studies, indicates that increasing productivity is a response to climate warming. However, our findings that greening was greatest within regions dominated by upright shrubs and within flat to gently sloping areas at moderate elevation suggests that the effects of temperature on tundra ecosystems are mediated by variation in microclimate and soil moisture, and physiological difference among plant functional types. Quantifying the response of tundra vegetation to warming is critical to our understanding of the feedbacks between ecosystems and the global climate system. To facilitate the development of predictive models, future research should combine process-oriented studies of tundra plant physiology with remote sensing studies across a range of spatial scales to identify the mechanisms that make some terrain types more sensitive to change than others.

Declaration of Competing Interest

None.

Acknowledgements

This research was funded by the Natural Sciences and Engineering Research Council of Canada (RGPIN 06210-2018: TCL), the University of Victoria, the Arctic Institute of North America (Lorraine Allison Scholarship: AC), the Northern Scientific Training Program and the Polar Continental Shelf Program. Data processing and analysis was partially enabled by the computational capabilities provided by WestGrid (www.westgrid.ca) and Compute Canada (computecanada.ca). Open access publication is supported by the Government of Canada. The authors would also like to thank Nicholas Coops, Gregory Rickbeil, David Swanson, Kiyo Campbell, Jordan Seider, Joe Antos, and Carissa Brown for discussions that informed this research as well as the editor and anonymous reviewers who provided constructive feedback and comments on earlier versions of our manuscript.

References

Agriculture and Agri-Food Canada, 2013. Terrestrial Ecoregions of Canada. https://sis.agr.gc.ca/cansis.

Berner, L.T., Beck, P.S.A., Bunn, A.G., Lloyd, A.H., Goetz, S.J., 2011. High-latitude tree growth and satellite vegetation indices: correlations and trends in Russia and Canada (1982–2008). J. Geophys. Res. 116, G01015 https://doi.org/10.1029/2010JG001475.

Bhatt, U., Walker, D., Raynolds, M., Bieniek, P., Epstein, H., Comiso, J., Pinzon, J., Tucker, C., Polyakov, I., 2013. Recent declines in warming and vegetation greening trends over pan-arctic tundra. Remote Sens. 5, 4229–4254. https://doi.org/10.3390/rs5094229.

Bhatt, U.S., Walker, D.A., Raynolds, M.K., Bieniek, P.A., Epstein, H.E., Comiso, J.C., Pinzon, J.E., Tucker, C.J., Steele, M., Ermold, W., Zhang, J., 2017. Changing seasonality of panarctic tundra vegetation in relationship to climatic variables. Environ. Res. Lett. 12 https://doi.org/10.1088/1748-9326/aa6b0b.

Bjorkman, A.D., Myers-Smith, I.H., Elmendorf, S.C., Normand, S., Rüger, N., Beck, P.S.A., Blach-Obergaard, A., Blok, D., Cornelissen, J.H.C., Forbes, B.C., Georges, D., Goetz, S.J., Guay, K.C., Henry, G.H.R., HilleRisLambers, J., Hollister, R.D., Karger, D. N., Kattge, J., Manning, P., Prevéy, J.S., Rixen, C., Schaepman-Strub, G., Thomas, H. J.D., Vellend, M., Wilmking, M., Wipf, S., et al., 2018. Plant functional trait change across a warming tundra biome. Nature 562, 57–62. https://doi.org/10.1038/s41586-018-0563-7.

Blok, D., Heijmans, M.M.P.D., Schaepman-Strub, G., Kononov, A.V., Maximov, T.C., Berendse, F., 2010. Shrub expansion may reduce summer permafrost thaw in Siberian tundra. Glob. Chang. Biol. 16 https://doi.org/10.1111/j.1365-2486.2009.02110.x.

Blok, D., Schaepman-Strub, G., Bartholomeus, H., Heijmans, M.P.D., Maximov, T.C., Berendse, F., 2011. The response of Arctic vegetation to the summer climate: relation between shrub cover, NDVI, surface albedo and temperature. Environ. Res. Lett. 6 https://doi.org/10.1088/1748-9326/6/3/035502.

Boelman, N.T., Gough, L., McLaren, J.R., Greaves, H., 2011. Does NDVI reflect variation in the structural attributes associated with increasing shrub dominance in arctic tundra? Environ. Res. Lett. 6, 035501 https://doi.org/10.1088/1748-9326/6/3/035501.

Bolton, D.K., Coops, N.C., Hermosilla, T., Wulder, M.A., White, J.C., 2018. Evidence of vegetation greening at alpine treeline ecotones: three decades of landsat spectral trends informed by lidar-derived vertical structure. Environ. Res. Lett. 13 https://doi.org/10.1088/1748-9326/aad5d2.

Bonney, M.T., Danby, R.K., Treitz, P.M., 2018. Landscape variability of vegetation change across the forest to tundra transition of central Canada. Remote Sens. Environ. 217 https://doi.org/10.1016/j.rse.2018.08.002.

Boudreau, S., Villeneuve-Simard, M.P., 2012. Dendrochronological evidence of shrub growth suppression by trees in a subarctic lichen woodland. Botany. https://doi.org/10.1139/B11-089.

Boulanger-Lapointe, N., Lévesque, E., Boudreau, S., Henry, G.H.R., Schmidt, N.M., 2014. Population structure and dynamics of Arctic willow (*Salix arctica*) in the High Arctic. J. Biogeogr. 41, 1967–1978. https://doi.org/10.1111/jbi.12350.

Boulesteix, A.L., Janitza, S., Kruppa, J., König, I.R., 2012. Overview of random forest methodology and practical guidance with emphasis on computational biology and bioinformatics. Wiley Interdiscip. Rev. Data Min. Knowl. Discov. 2, 493–507. https://doi.org/10.1002/widm.1072.

Breiman, L., 2001. Random Forests. Mach. Learn. 45, 5–32. https://doi.org/10.1023/A:1010933404324.

Bret-Harte, S.M., Shaver, G.R., Zoerner, J.P., Johnstone, J.F., Wagner, J.L., Chavez, A.S., Gunkelman Iv, R.F., Lippert, S.C., Laundre, J.A., 2001. Developmental plasticity allows betula nana to dominate tundra subjected to an altered environment. Ecology. https://doi.org/10.1890/0012-9658(2001)082[0018:DPABNT]2.0.CO;2.

Bret-Harte, M.S., Mack, M.C., Shaver, G.R., Huebner, D.C., Johnston, M., Mojica, C.A., Pizano, C., Reiskind, J.A., 2013. The response of Arctic vegetation and soils following an unusually severe tundra fire. Philos. Trans. R. Soc. B Biol. Sci. 368 https://doi.org/10.1098/rstb.2012.0490.

Bunn, A.G., Goetz, S.J., Bunn, A.G., Goetz, S.J., 2006. Trends in satellite-observed circumpolar photosynthetic activity from 1982 to 2003: the influence of seasonality, cover type, and vegetation density. Earth Interact. 10, 1–19. https://doi.org/10.1175/EI190.1.

Burn, C.R., Kokelj, S.V., 2009. The environment and permafrost of the Mackenzie Delta area. Permafr. Periglac. Process. 20, 83–105. https://doi.org/10.1002/ppp.655.

Cameron, E.A., Lantz, T.C., 2016. Drivers of tall shrub proliferation adjacent to the Dempster Highway, Northwest Territories, Canada. Environ. Res. Lett. 11 https://doi.org/10.1088/1748-9326/11/4/045006.

Campbell, T.K.F., Lantz, T.C., Fraser, R.H., Hogan, D., 2020. High arctic vegetation change mediated by hydrological conditions. Ecosystems. https://doi.org/10.1007/s10021-020-00506-7.

Chapin, F.S., Sturm, M., Serreze, M.C., McFadden, J.P., Key, J.R., Lloyd, A.H., McGuire, A.D., Rupp, T.S., Lynch, A.H., Schimel, J.P., Beringer, J., Chapman, W.L., Epstein, H.E., Euskirchen, E.S., Hinzman, L.D., Jia, G., Ping, C.L., Tape, K.D., Thompson, C.D.C., Walker, D.A., Welker, J.M., 2005. Role of land-surface changes in arctic summer warming. Science (80-.) 310, 657–660. https://doi.org/10.1126/science.1117368.

Christiansen, C.T., Lafreniére, M.J., Henry, G.H.R., Grogan, P., 2018. Long-term deepened snow promotes tundra evergreen shrub growth and summertime ecosystem net CO2 gain but reduces soil carbon and nutrient pools. Glob. Chang. Biol. 24, 3508–3525. https://doi.org/10.1111/gcb.14084.

Cowtan, K., Way, R.G., 2014. Coverage bias in the HadCRUT4 temperature series and its impact on recent temperature trends. Q. J. R. Meteorol. Soc. 140, 1935–1944. https://doi.org/10.1002/qj.2297.

de Beurs, K.M., Henebry, G.M., Owsley, B.C., Sokolik, I., 2015. Using multiple remote sensing perspectives to identify and attribute land surface dynamics in Central Asia 2001–2013. Remote Sens. Environ. 170, 48–61. https://doi.org/10.1016/j.rse.2015.08.018.

de Jong, R., Verbesselt, J., Zeileis, A., Schaepman, M., 2013. Shifts in global vegetation activity trends. Remote Sens. 5, 1117–1133. https://doi.org/10.3390/rs5031117.

Dearborn, K.D., Danby, R.K., 2017. Aspect and slope influence plant community composition more than elevation across forest-tundra ecotones in subarctic Canada. J. Veg. Sci. 28, 595–604. https://doi.org/10.1111/jvs.12521.

Drake, T.W., Holmes, R.M., Zhulidov, A.V., Gurtovaya, T., Raymond, P.A., McClelland, J. W., Spencer, R.G.M., 2019. Multidecadal climate-induced changes in Arctic tundra lake geochemistry and geomorphology. Limnol. Oceanogr. 64, S179–S191. https://doi.org/10.1002/lno.11015.

Ecosystem Classification Group, 2013. Ecological Regions of the Northwest Territories - Northern Arctic. Yellowknife.

Edwards, R., Treitz, P., 2017. Vegetation greening trends at two sites in the Canadian Arctic. Arctic Antarct. Alp. Res. 49, 601–619. https://doi.org/10.1657/AAAR0016-075.

Elmendorf, S.C., Henry, G.H.R., Hollister, R.D., 2012a. Plot-scale evidence of tundra vegetation change and links to recent summer warming. Nat. Clim. Chang. 2 https://doi.org/10.1038/NCLIMATE1465.

Elmendorf, S.C., Henry, G.H.R., Hollister, R.D., Björk, R.G., Bjorkman, A.D., Callaghan, T.V., Collier, L.S., Cooper, E.J., Cornelissen, J.H.C., Day, T.A., Fosaa, A. M., Gould, W.A., Grétarsdóttir, J., Harte, J., Hermanutz, L., Hik, D.S., Hofgaard, A., Jarrad, F., Jónsdóttir, I.S., Keuper, F., Klanderud, K., Klein, J.A., Koh, S., Kudo, G., Lang, S.I., Loewen, V., May, J.L., Mercado, J., Michelsen, A., Molau, U., Myers-Smith, I.H., Oberbauer, S.F., Pieper, S., Post, E., Rixen, C., Robinson, C.H., Schmidt, N.M., Shaver, G.R., Stenström, A., Tolvanen, A., Totland, Ø., Troxler, T., Wahren, C.H., Webber, P.J., Welker, J.M., Wookey, P.A., 2012b. Global assessment of experimental climate warming on tundra vegetation: heterogeneity over space and time. Ecol. Lett. https://doi.org/10.1111/j.1461-0248.2011.01716.x.

Elmendorf, S.C., Henry, G.H.R., Hollister, R.D., Fosaa, A.M., Gould, W.A., Hermanutz, L., Hofgaard, A., Jónsdóttir, I.S., Jónsdóttir, I.I., Jorgenson, J.C., Lévesque, E., Magnusson, B., Molau, U., Myers-Smith, I.H., Oberbauer, S.F., Rixen, C., Tweedie, C. E., Walker, M.D., Walker, M., 2015. Experiment, monitoring, and gradient methods used to infer climate change effects on plant communities yield consistent patterns. Proc. Natl. Acad. Sci. U. S. A. 112, 448–452. https://doi.org/10.1073/pnas.1410088112.

Epstein, H.E., Walker, D.A., Raynolds, M.K., Jia, G.J., Kelley, A.M., 2008. Phytomass patterns across a temperature gradient of the North American arctic tundra. J. Geophys. Res. 113, G03S02 https://doi.org/10.1029/2007JG000555.

Evans, J.S., 2020. spatialEco: Spatial Analysis and Modelling Utilities.

Fisher, J.I., Mustard, J.F., 2007. Cross-scalar satellite phenology from ground, Landsat, and MODIS data. Remote Sens. Environ. 109, 261–273. https://doi.org/10.1016/j.rse.2007.01.004.

Foody, G.M., 2009. Classification accuracy comparison: hypothesis tests and the use of confidence intervals in evaluations of difference, equivalence and non-inferiority. Remote Sens. Environ. 113, 1658–1663. https://doi.org/10.1016/j.rse.2009.03.014.

Fraser, R.H., Lantz, T.C., Olthof, I., Kokelj, S.V., Sims, R.A., 2014. Warming-induced shrub expansion and lichen decline in the Western Canadian Arctic. Ecosystems 17, 1151–1168. https://doi.org/10.1007/s10021-014-9783-3.

Fraser, R.H., Olthof, I., Lantz, T.C., Schmitt, C., 2016. UAV photogrammetry for mapping vegetation in the low-Arctic. Arct. Sci. 2, 79–102. https://doi.org/10.1139/as-2016-0008.

Frost, G.V., Epstein, H.E., Walker, D.A., Matyshak, G., Ermokhina, K., 2018. Seasonal and long-term changes to active-layer temperatures after tall shrubland expansion and succession in Arctic tundra. Ecosystems 21, 507–520. https://doi.org/10.1007/s10021-017-0165-5.

Fulton, R.J., 1989. Quaternary geology of Canada and Greenland. Quat. Geol. Canada Greenl. https://doi.org/10.1130/dnag-gna-k1.

Goetz, S., Campbell, E., Euskirchen, E.S., Poulter, B., 2019. Trends and Drivers of Greening and Browning. Understanding Northern Latitude Vegetation Greening and Browning. National Academies Press, Washington, DC, pp. 7–14. https://doi.org/10.17226/25423.

Greaves, H.E., Vierling, L.A., Eitel, J.U.H., Boelman, N.T., Magney, T.S., Prager, C.M., Griffin, K.L., 2016. High-resolution mapping of aboveground shrub biomass in Arctic tundra using airborne lidar and imagery. Remote Sens. Environ. 184 https://doi.org/10.1016/j.rse.2016.07.026.

Guay, K.C., Beck, P.S.A., Berner, L.T., Goetz, S.J., Baccini, A., Buermann, W., 2014. Vegetation productivity patterns at high northern latitudes: a multi-sensor satellite data assessment (supporting figures). Glob. Chang. Biol. 20, 3147–3158. https://doi.org/10.1111/gcb.12647.

Hansen, B.B., Isaksen, K., Benestad, R.E., Kohler, J., Pedersen, Å., Loe, L.E., Coulson, S.J., Larsen, J.O., Varpe, Ø., 2014. Warmer and wetter winters: characteristics and implications of an extreme weather event in the High Arctic. Environ. Res. Lett. 9 https://doi.org/10.1088/1748-9326/9/11/114021.

Harris, I., Jones, P.D., Osborn, T.J., Lister, D.H., 2014. Updated high-resolution grids of monthly climatic observations - the CRU TS3.10 Dataset. Int. J. Climatol. 34, 623–642. https://doi.org/10.1002/joc.3711.

Harris, I., Osborn, T.J., Jones, P., Lister, D., 2020. Version 4 of the CRU TS monthly high-resolution gridded multivariate climate dataset. Sci. Data 7, 1–18. https://doi.org/10.1038/s41597-020-0453-3.

Hermosilla, T., Wulder, M.A., White, J.C., Coops, N.C., Hobart, G.W., 2015. An integrated Landsat time series protocol for change detection and generation of annual gap-free surface reflectance composites. Remote Sens. Environ. 158, 220–234. https://doi.org/10.1016/j.rse.2014.11.005.

Hermosilla, T., Wulder, M.A., White, J.C., Coops, N.C., Hobart, G.W., Campbell, L.C., 2016. Mass data processing of time series Landsat imagery: pixels to data products for forest monitoring. Int. J. Digit. Earth. https://doi.org/10.1080/17538947.2016.1187673.

Huete, A., Didan, K., Miura, T., Rodriguez, E.P., Gao, X., Ferreira, L.G., 2002. Overview of the radiometric and biophysical performance of the MODIS vegetation indices. Remote Sens. Environ. 83, 195–213. https://doi.org/10.1016/S0034-4257(02)00096-2.

Jeong, J.H., Resop, J.P., Mueller, N.D., Fleisher, D.H., Yun, K., Butler, E.E., Timlin, D.J., Shim, K.-M., Gerber, J.S., Reddy, V.R., Kim, S.-H., 2016. Random Forests for global and regional crop yield predictions. PLoS One 11, e0156571. https://doi.org/10.1371/journal.pone.0156571.

Jia, G.J., Epstein, H.E., Walker, D.A., 2009. Vegetation greening in the canadian arctic related to decadal warming. J. Environ. Monit. 11, 2231–2238. https://doi.org/10.1039/b911677j.

Jorgenson, J.C., Jorgenson, M.T., Boldenow, M.L., Orndahl, K.M., 2018a. Landscape change detected over a half century in the Arctic National Wildlife Refuge using high-resolution aerial imagery. Remote Sens. 10, 1305. https://doi.org/10.3390/RS10081305.

Jorgenson, M., Frost, G., Dissing, D., 2018b. Drivers of landscape changes in coastal ecosystems on the Yukon-Kuskokwim Delta, Alaska. Remote Sens. 10, 1280. https://doi.org/10.3390/rs10081280.

Ju, J., Masek, J.G., 2016. The vegetation greenness trend in Canada and US Alaska from 1984–2012 Landsat data. Remote Sens. Environ. 176, 1–16. https://doi.org/10.1016/J.RSE.2016.01.001.

Kuhn, M., 2020. caret: Classification and Regression Training.

Kushida, K., Hobara, S., Tsuyuzaki, S., Kim, Y., Watanabe, M., Setiawan, Y., Harada, K., Shaver, G.R., Fukuda, M., 2015. Spectral indices for remote sensing of phytomass, deciduous shrubs, and productivity in Alaskan Arctic tundra. Int. J. Remote Sens. 36, 4344–4362. https://doi.org/10.1080/01431161.2015.1080878.

Kwon, H.J., Oechel, W.C., Zulueta, R.C., Hastings, S.J., 2006. Effects of climate variability on carbon sequestration among adjacent wet sedge tundra and moist tussock tundra ecosystems. J. Geophys. Res. Biogeosci. 111 https://doi.org/10.1029/2005JG000036.

Lakens, D., 2017. Equivalence Tests: A Practical Primer for t Tests, Correlations, and Meta-analyses. https://doi.org/10.1177/1948550617697177.

Lantz, T.C., Marsh, P., Kokelj, S.V., 2013. Recent shrub proliferation in the Mackenzie Delta uplands and microclimatic implications. Ecosystems 16, 47–59. https://doi.org/10.1007/s10021-012-9595-2.

Lantz, T.C., Gergel, S.E., Kokelj, S.V., 2010. Spatial Heterogeneity in the Shrub Tundra Ecotone in the Mackenzie Delta Region, Northwest Territories: Implications for Arctic Environmental Change. Ecosystems 13 (2), 194–204. https://doi.org/10.1007/s10021-009-9310-0.

Lantz, T.C., Kokelj, S.V., Fraser, R.H., 2015. Ecological recovery in an Arctic delta following widespread saline incursion. Ecol. Appl. 25, 172–185. https://doi.org/10.1890/14-0239.1.

Liaw, A., Wiener, M., 2018. randomForest: Breiman and Cutler's Random Forests for Classification and Regression.

Liljedahl, A.K., Boike, J., Daanen, R.P., Fedorov, A.N., Frost, G.V., Grosse, G., Hinzman, L.D., Iijma, Y., Jorgenson, J.C., Matveyeva, N., Necsoiu, M., Raynolds, M. K., Romanovsky, V.E., Schulla, J., Tape, K.D., Walker, D.A., Wilson, C.J., Yabuki, H., Zona, D., 2016. Pan-Arctic ice-wedge degradation in warming permafrost and its influence on tundra hydrology. Nat. Geosci. 9, 312–318. https://doi.org/10.1038/ngeo2674.

Liu, N., Treitz, P., 2018. Remote sensing of Arctic percent vegetation cover and fAPAR on Baffin Island, Nunavut, Canada. Int. J. Appl. Earth Obs. Geoinf. 71, 159–169. https://doi.org/10.1016/j.jag.2018.05.011.

Loranty, M.M., Lieberman-Cribbin, W., Berner, L.T., Natali, S.M., Goetz, S.J., Alexander, H.D., Kholodov, A.L., 2016. Spatial variation in vegetation productivity trends, fire disturbance, and soil carbon across arctic-boreal permafrost ecosystems. Environ. Res. Lett. https://doi.org/10.1088/1748-9326/11/9/095008.

Mann, H.B., 1945. Nonparametric Tests Against Trend. Econometrica 13, 245. https://doi.org/10.2307/1907187.

Marsh, P., Bartlett, P., MacKay, M., Pohl, S., Lantz, T., 2010. Snowmelt energetics at a shrub tundra site in the western Canadian Arctic. Hydrological Processes 24 (25), 3603–3620. https://doi.org/10.1002/hyp.7786.

Martin, A., Jeffers, E., Petrokofsky, G., Myers-Smith, I., Macias-Fauria, M., 2017. Shrub growth and expansion in the Arctic tundra: an assessment of controlling factors using an evidence-based approach. Environ. Res. Lett. 12.

Mcguire, A.D., Anderson, L.G., Christensen, T.R., Scott, D., Laodong, G., Hayes, D.J., Martin, H., Lorenson, T.D., Macdonald, R.W., Nigel, R., 2009. Sensitivity of the carbon cycle in the Arctic to climate change. Ecol. Monogr. https://doi.org/10.1890/08-2025.1.

McLeod, A.I., 2011. Kendall: Kendall Rank Correlation and Mann-Kendall Trend Test.

McManus, K.M., Morton, D.C., Masek, J.G., Wang, D., Sexton, J.O., Nagol, J.R., Ropars, P., Boudreau, S., 2012. Satellite-based evidence for shrub and graminoid tundra expansion in northern Quebec from 1986 to 2010. Glob. Chang. Biol. 18, 2313–2323. https://doi.org/10.1111/j.1365-2486.2012.02708.x.

Meredith, M., Sommerkorn, M., Cassotta, S., Derksen, C., Ekaykin, A, Hallowed, A, Kofinas, G., Mackintosh, A., Melbourne-Thomas, J., Muelbert, M.M.C., Otterson, G., Pritchard, H., Schuur, E.A.G., 2019. Chapter 3: polar regions. Special Report on the Ocean and Cryosphere in a Changing Climate. Intergovernmental Panel on Climate Change.

Moffat, N.D., Lantz, T.C., Fraser, R.H., Olthof, I., 2016. Recent vegetation change (1980–2013) in the tundra ecosystems of the Tuktoyaktuk Coastlands, NWT, Canada. Arctic Antarct. Alp. Res. https://doi.org/10.1657/AAAR0015-063.

Myers-Smith, I.H., Hik, D.S., 2018. Climate warming as a driver of tundra shrubline advance. J. Ecol. 106, 547–560. https://doi.org/10.1111/1365-2745.12817.

Myers-Smith, I.H., Forbes, B.C., Wilmking, M., Hallinger, M., Lantz, T., Blok, D., Tape, K. D., Macias-Fauria, M., Sass-Klaassen, U., Lévesque, E., Boudreau, S., Ropars, P., Hermanutz, L., Trant, A., Collier, L.S., Weijers, S., Rozema, J., Rayback, S.A., Schmidt, N.M., Schaepman-Strub, G., Wipf, S., Rixen, C., Ménard, C.B., Venn, S., Goetz, S., Andreu-Hayles, L., Elmendorf, S., Ravolainen, V., Welker, J., Grogan, P., Epstein, H.E., Hik, D.S., 2011a. Shrub expansion in tundra ecosystems: dynamics, impacts and research priorities. Environ. Res. Lett. 6, 045509 https://doi.org/10.1088/1748-9326/6/4/045509.

Myers-Smith, I.H., Hik, D.S., Kennedy, C., Cooley, D., Johnstone, J.F., Kenney, A.J., Krebs, C.J., 2011b. Expansion of canopy-forming willows over the twentieth century on Herschel Island, Yukon Territory, Canada. Ambio 40, 610–623. https://doi.org/10.1007/s13280-011-0168-y.

Myers-Smith, I.H., Elmendorf, S.C., Beck, P.S.A., Wilmking, M., Hallinger, M., Blok, D., Tape, K.D., Rayback, S.A., Macias-Fauria, M., Forbes, B.C., Speed, J.D.M., Boulanger-Lapointe, N., Rixen, C., Lévesque, E., Schmidt, N.M., Baittinger, C., Trant, A.J., Hermanutz, L., Collier, L.S., Dawes, M.A., Lantz, T.C., Weijers, S., JØrgensen, R.H., Buchwal, A., Buras, A., Naito, A.T., Ravolainen, V., Schaepman-Strub, G., Wheeler, J. A., Wipf, S., Guay, K.C., Hik, D.S., Vellend, M., 2015. Climate sensitivity of shrub growth across the tundra biome. Nat. Clim. Chang. 5, 887–891. https://doi.org/10.1038/nclimate2697.

Myers-Smith, I.H., Grabowski, M.M., Thomas, H.J.D., Angers-Blondin, S., Daskalova, G. N., Bjorkman, A.D., Cunliffe, A.M., Assmann, J.J., Boyle, J.S., McLeod, E., McLeod, S., Joe, R., Lennie, P., Arey, D., Gordon, R.R., Eckert, C.D., 2019. Eighteen years of ecological monitoring reveals multiple lines of evidence for tundra vegetation change. Ecol. Monogr. 89, e01351 https://doi.org/10.1002/ecm.1351.

Myers-Smith, I.H., Kerby, J.T., Phoenix, G.K, Bjerke, J.W., Epstein, H.E., Assmann,, J.J., John, C., Andreu-Hayles, L., Angers-Blondin, S., Beck, P.S.A., Berner, L.T., Bhatt, U. S., Bjorkman, A.D., Blok, D., Christiansen, C.T., Hans, J., Cornelissen, C., Cunliffe, A. M., Elmendorf, S.C., Forbes, B.C., Goetz, S.J., Hollister, R.D., de Jong, R., Loranty, M. M., Macias-Fauria, M., Maseyk, K., Normand, S., Olofsson, J., Parker, T.C., Permentier, F.J.W., Schaepman-Strub, G., Stordal, F., Sullivan, P.F., Thomas, H.J.D., Tømmervik, H., Treharne, R., Tweedie, C.E., Walker, D.A., Wilmking, M., Wipf, S., 2020. Complexity revealed in the greening of the Arctic. Nature Climate Change 10, 106–117. https://doi.org/10.1038/s41558-019-0688-1.

Natural Resources Canada, 2015. Canadian Digital Elevation Model, 1945-2011. https://open.canada.ca/data/en/dataset/7f245e4d-76c2-4caa-951a-45d1d2051333.

Oberbauer, S.F., Tweedie, C.E., Welker, J.M., Fahnestock, J.T., Henry, G.H.R., Webber, P. J., Hollister, R.D., Walker, M.D., Kuchy, A., Elmore, E., Starr, G., 2007. Tundra CO2 fluxes in response to experimental warming across latitudinal and moisture gradients. Ecol. Monogr. 77, 221–238. https://doi.org/10.1890/06-0649.

Ohse, B., Ohse, B., Jansen, F., Wilmking, M., 2012. Do limiting factors at Alaskan treelines shift with climatic regimes? Environ. Res. Lett. 7 https://doi.org/10.1088/1748-9326/7/1/015505.

Olthof, I., Fraser, R.H., 2007. Mapping northern land cover fractions using Landsat ETM +. Remote Sens. Environ. 107, 496–509. https://doi.org/10.1016/j.rse.2006.10.009.

Olthof, I., Latifovic, R., Pouliot, D., 2009. Development of a circa 2000 land cover map of northern canada at 30 m resolution from landsat. Can. J. Remote Sens. 35, 152–165. https://doi.org/10.5589/m09-007.

Overland, J.E., Wang, M., 2016. Recent extreme arctic temperatures are due to a split polar vortex. J. Clim. 29, 5609–5616. https://doi.org/10.1175/JCLI-D-16-0320.1.

Pedlar, J.H., McKenney, D.W., Lawrence, K., Papadopol, P., Hutchinson, M.F., Price, D., 2015. A comparison of two approaches for generating spatial models of growing-season variables for Canada. J. Appl. Meteorol. Climatol. 54, 506–518. https://doi.org/10.1175/JAMC-D-14-0045.1.

Phoenix, G.K., Bjerke, J.W., 2016. Arctic browning: extreme events and trends reversing arctic greening. Glob. Chang. Biol. 22, 2960–2962. https://doi.org/10.1111/gcb.13261.

Pithan, F., Mauritsen, T., 2014. Arctic amplification dominated by temperature feedbacks in contemporary climate models. Nat. Geosci. 7, 181–184. https://doi.org/10.1038/ngeo2071.

Raynolds, M.K., Walker, D.A., 2009. Effects of deglaciation on circumpolar distribution of arctic vegetation. Can. J. Remote Sens. 35, 118–129. https://doi.org/10.5589/m09-006.

Raynolds, M.K., Walker, D.A., 2016. Increased wetness confounds Landsat-derived NDVI trends in the central Alaska North Slope region, 1985–2011. Environ. Res. Lett. 11, 085004 https://doi.org/10.1088/1748-9326/11/8/085004.

Raynolds, M.K., Walker, D.A., Maier, H.A., 2006. NDVI patterns and phytomass distribution in the circumpolar Arctic. Remote Sens. Environ. 102, 271–281. https://doi.org/10.1016/j.rse.2006.02.016.

Raynolds, M.K., Comiso, J.C., Walker, D.A., Verbyla, D., 2008. Relationship between satellite-derived land surface temperatures, arctic vegetation types, and NDVI. Remote Sens. Environ. 112, 1884–1894. https://doi.org/10.1016/j.rse.2007.09.008.

R Core Team, 2013. R: A Language and Environment for Statistical Computing. https://www.r-project.org/.

Reichle, L.M., Epstein, H.E., Bhatt, U.S., Raynolds, M.K., Walker, D.A., 2018. Spatial heterogeneity of the temporal dynamics of Arctic tundra vegetation. Geophys. Res. Lett. 45, 9206–9215. https://doi.org/10.1029/2018GL078820.

Rickbeil, G.J.M., Hermosilla, T., Coops, N.C., White, J.C., Wulder, M.A., Lantz, T.C., 2018. Changing northern vegetation conditions are influencing barren ground caribou (Rangifer tarandus groenlandicus) post-calving movement rates. J. Biogeogr. 45, 702–712. https://doi.org/10.1111/jbi.13161.
Roberts, D.W., Coopers, S.V., 1989. Concepts and techniques of vegetation mapping. Land classifications based on vegetation: applications for resource management, GTR-INT-257. USDA Forest Service Intermountain Research Station, Ogden, UT, pp. 90–96.
Rocha, A.V., Blakely, B., Jiang, Y., Wright, K.S., Curasi, S.R., 2018. Is arctic greening consistent with the ecology of tundra? Lessons from an ecologically informed mass balance model. Environ. Res. Lett. 13, 125007. https://doi.org/10.1088/1748-9326/aaeb50.
Ropars, P., Boudreau, S., 2012. Shrub expansion at the foresttundra ecotone: spatial heterogeneity linked to local topography. Environ. Res. Lett. 7 https://doi.org/10.1088/1748-9326/7/1/015501.
Ropars, P., Lévesque, E., Boudreau, S., 2015. How do climate and topography influence the greening of the forest-tundra ecotone in northern Québec? A dendrochronological analysis of *Betula glandulosa*. J. Ecol. 103, 679–690. https://doi.org/10.1111/1365-2745.12394.
Roser, L., Vilardi, J., Saidman, B., Ferreyra, L., 2020. EcoGenetics: Management and Exploratory Analysis of Spatial Data in Landscape Genetics.
Rozema, J., Weijers, S., Broekman, R., Blokker, P., Buizer, B., Werleman, C., El Yaqine, H., Hoogedoorn, H., Fuertes, M.M., Cooper, E., 2009. Annual growth of Cassiope tetragona as a proxy for Arctic climate: developing correlative and experimental transfer functions to reconstruct past summer temperature on a millennial time scale. Glob. Chang. Biol. 15, 1703–1715. https://doi.org/10.1111/j.1365-2486.2009.01858.x.
Schaefer, K., Zhang, T., Bruhwiler, L., Barrett, A.P., 2011. Amount and timing of permafrost carbon release in response to climate warming. Chem. Phys. Meteorol. 63, 165–180. https://doi.org/10.1111/j.1600-0889.2010.00527.x.
Schut, A.G.T., Ivits, E., Conijn, J.G., ten Brink, B., Fensholt, R., 2015. Trends in global vegetation activity and climatic drivers indicate a decoupled response to climate change. PLoS One 10, e0138013. https://doi.org/10.1371/journal.pone.0138013.
Schuur, E.A.G., McGuire, A.D., Schädel, C., Grosse, G., Harden, J.W., Hayes, D.J., Hugelius, G., Koven, C.D., Kuhry, P., Lawrence, D.M., Natali, S.M., Olefeldt, D., Romanovsky, V.E., Schaefer, K., Turetsky, M.R., Treat, C.C., Vonk, J.E., 2015. Climate change and the permafrost carbon feedback. Nature. https://doi.org/10.1038/nature14338.
Sen, P.K., 1968. Estimates of the regression coefficient based on Kendall's tau. J. Am. Stat. Assoc. 63, 1379–1389. https://doi.org/10.1080/01621459.1968.10480934.
Serreze, M.C., Walsh, J.E., Chapin, F.S., Osterkamp, T., Dyurgerov, M., Romanovsky, V., Oechel, W.C., Morison, J., Zhang, T., Barry, R.G., 2000. Observational evidence of recent change in the northern high-latitude environment. Clim. Change 46, 159–207. https://doi.org/10.1023/A:1005504031923.
Shaver, G.R., Bret-Harte, S.M., Jones, M.H., Johnstone, J., Gough, L., Laundre, J., Chapin, C.F., 2001. Species composition interacts with fertilizer to control long-term change in tundra productivity. Ecology 82 (11), 3163–3181. https://doi.org/10.1890/0012-9658(2001)082[3163:SCIWFT]2.0.CO;2.
Silapaswan, C.S., Verbyla, D.L., Mc Guire, A.D., 2001. Land cover change on the seward peninsula: the use of remote sensing to evaluate the potential influences of climate warming on historical vegetation dynamics. Can. J. Remote Sens. 27, 542–554. https://doi.org/10.1080/07038992.2001.10854894.
Smith, C.A.S., Meikle, J.C., Roots, C.F., 2004. Ecoregions of the Yukon Territory: Biophysical Properties of Yukon Landscapes. Summerland, BC.
Stocker, T.F., Qin, D., Plattner, G.-K., Tignor, M.M.B., Allen, S.K., Boschung, J., Nauels, A., Xia, Y., Bex, V., Midgley, P.M., 2013. The Physical Science Basis: Working Group I Contribution to the Fifth Assessment Report of the Intergovernmental Panel on Climate Change.
Sulla-Menashe, D., Woodcock, C.E., Friedl, M.A., 2018. Canadian boreal forest greening and browning trends: an analysis of biogeographic patterns and the relative roles of disturbance versus climate drivers. Environ. Res. Lett. 13 https://doi.org/10.1088/1748-9326/aa9b88.
Svoboda, J., Henry, R., 1987. Succession in marginal Arctic environments. Arct. Alp. Res. 19, 373–384. https://doi.org/10.1080/00040851.1987.12002618.
Swanson, D., 2017. Trends in greenness and snow cover in Alaska's Arctic National Parks, 2000–2016. Remote Sens. 9, 514. https://doi.org/10.3390/rs9060514.
Tape, K.D., Hallinger, M., Welker, J.M., Ruess, R.W., 2012. Landscape heterogeneity of shrub expansion in Arctic Alaska. Ecosystems 15, 711–724. https://doi.org/10.1007/s10021-012-9540-4.
Tarnocai, C., 2004. Classification of cryosols in Canada. In: Cryosols. Springer, Berlin Heidelberg, pp. 599–610. https://doi.org/10.1007/978-3-662-06429-0_30.
Timoney, K.P., La Roi, G.H., Zoltai, S.C., Robinson, A.L., 1992. The high subarctic forest-tundra of northwestern Canada: position, width, and vegetation gradients in relation to climate. Arctic 45, 1–9. https://doi.org/10.14430/arctic1367.
Travers-Smith, H., Lantz, T.C., 2020. Leading edge disequilibrium in sub-Arctic alder and spruce populations. Ecosphere 11 (7), e03118.
Tremblay, B., Lévesque, E., Boudreau, S., 2012. Recent expansion of erect shrubs in the Low Arctic: evidence from Eastern Nunavik. Environ. Res. Lett. 7, 035501 https://doi.org/10.1088/1748-9326/7/3/035501.
Tsuyuzaki, S., Iwahana, G., Saito, K., 2017. Tundra fire alters vegetation patterns more than the resultant thermokarst. Polar Biol. 1–9. https://doi.org/10.1007/s00300-017-2236-7.
Tunes da Silva, G., Logan, B.R., Klein, J.P., 2009. Methods for equivalence and noninferiority testing. Biol. Blood Marrow Transplant. 15, 120–127. https://doi.org/10.1016/j.bbmt.2008.10.004.
Van Hemert, C., Flint, P.L., Udevitz, M.S., Koch, J.C., Atwood, T.C., Oakley, K.L., Pearce, J.M., 2015. Forecasting wildlife response to rapid warming in the Alaskan Arctic. Bioscience. https://doi.org/10.1093/biosci/biv069.
Verbyla, D., 2011. Browning boreal forests of western North America. Environ. Res. Lett. 6, 041003 https://doi.org/10.1088/1748-9326/6/4/041003.
Vermaire, J.C., Pisaric, M.F.J., Thienpont, J.R., Courtney Mustaphi, C.J., Kokelj, S.V., Smol, J.P., 2013. Arctic climate warming and sea ice declines lead to increased storm surge activity. Geophys. Res. Lett. 40, 1386–1390. https://doi.org/10.1002/grl.50191.
Vincent, L.A., Zhang, X., Brown, R.D., Feng, Y., Mekis, E., Milewska, E.J., Wan, H., Wang, X.L., 2015. Observed trends in Canada's climate and influence of low-frequency variability modes. J. Clim. 28, 4545–4560. https://doi.org/10.1175/JCLI-D-14-00697.1.
Wahren, C.H.A., Walker, M.D., Bret-Harte, M.S., 2005. Vegetation responses in Alaskan arctic tundra after 8 years of a summer warming and winter snow manipulation experiment. Glob. Chang. Biol. 11, 537–552. https://doi.org/10.1111/j.1365-2486.2005.00927.x.
Walker, D.A., Raynolds, M.K., Daniëls, F.J.A., Einarsson, E., Elvebakk, A., Gould, W.A., Katenin, A.E., Kholod, S.S., Markon, C.J., Melnikov, E.S., Moskalenko, N.G., Talbot, S.S., Yurtsev, B.A., The other members of the CAVM Team, 2005. The Circumpolar Arctic vegetation map. J. Veg. Sci. 16, 267–282. https://doi.org/10.1111/j.1654-1103.2005.tb02365.x.
Walker, M.D., Wahren, C.H., Hollister, R.D., Henry, G.H.R., Ahlquist, L.E., Alatalo, J.M., Bret-Harte, M.S., Calef, M.P., Callaghan, T.V., Carroll, A.B., Epstein, H.E., Jónsdóttir, I.S., Klein, J.A., Magnússon, B., Molau, U., Oberbauer, S.F., Rewa, S.P., Robinson, C.H., Shaver, G.R., Suding, K.N., Thompson, C.C., Tolvanen, A., Totland, Ø., Turner, P.L., Tweedie, C.E., Webber, P.J., Wookey, P.A., 2006. Plant community responses to experimental warming across the tundra biome. Proc. Natl. Acad. Sci. U. S. A. 103, 1342–1346. https://doi.org/10.1073/pnas.0503198103.
Weijers, S., Buchwal, A., Blok, D., Löffler, J., Elberling, B., 2017. High Arctic summer warming tracked by increased *Cassiope tetragona* growth in the world's northernmost polar desert. Glob. Chang. Biol. 23, 5006–5020. https://doi.org/10.1111/gcb.13747.
Weston, S., 2019. doParallel: Foreach Parallel Adaptor for the "parallel" Package.
Weston, S., 2020. foreach: Provides Foreach Looping Construct.
White, J.C., Wulder, M.A., Hobart, G.W., Luther, J.E., Hermosilla, T., Griffiths, P., Coops, N.C., Hall, R.J., Hostert, P., Dyk, A., Guindon, L., White, J.C., 2014. Pixel-based image compositing for large-area dense time series applications and science. Can. J. Remote Sens. 40, 192–212. https://doi.org/10.1080/07038992.2014.945827.
Wickham, H., Averick, M., Bryan, J., Chang, W., McGowan, L.D., François, R., Grolemund, G., Hayes, A., Henry, L., Hester, J., Kuhn, M., Pedersen, T.L., Miller, E., Bache, S.M., Müller, K., Ooms, J., Robinson, D., Seidel, D.P., Spinu, V., Takahashi, K., Vaughan, D., Wilke, C., Woo, K., Yutani, H., 2019. Welcome to the {tidyverse}. J. Open Source Softw. 4, 1686 https://doi.org/10.21105/joss.01686.
Wickham, H., François, R., Henry, L., Müller, K., 2020. dplyr: A Grammar of Data Manipulation.
Wilcox, R.R., 1998. A note on the Theil-Sen regression estimator when the regresser is random and the error term is heteroscedastic. Biometr. J. 40, 261–268. https://doi.org/10.1002/(SICI)1521-4036(199807)40:3<261::AID-BIMJ261>3.0.CO;2-V.
Wilcox, E.J., Keim, D., de Jong, T., Walker, B., Sonnentag, O., Sniderhan, A.E., Mann, P., Marsh, P., 2019. Tundra shrub expansion may amplify permafrost thaw by advancing snowmelt timing. Arct. Sci. 5, 202–217. https://doi.org/10.1139/as-2018-0028.
Wolter, J., Lantuit, H., Herzschuh, U., Stettner, S., Fritz, M., 2017. Tundra vegetation stability versus lake-basin variability on the Yukon Coastal Plain (NW Canada) during the past three centuries. Holocene 27, 1846–1858. https://doi.org/10.1177/0959683617708441.
Wulder, M.A., Loveland, T.R., Roy, D.P., Crawford, C.J., Masek, J.G., Woodcock, C.E., Allen, R.G., Anderson, M.C., Belward, A.S., Cohen, W.B., Dwyer, J., Erb, A., Gao, F., Griffiths, P., Helder, D., Hermosilla, T., Hipple, J.D., Hostert, P., Hughes, M.J., Huntington, J., Johnson, D.M., Kennedy, R., Kilic, A., Li, Z., Lymburner, L., McCorkel, J., Pahlevan, N., Scambos, T.A., Schaaf, C., Schott, J.R., Sheng, Y., Storey, J., Vermote, E., Vogelmann, J., White, J.C., Wynne, R.H., Zhu, Z., 2019. Current status of Landsat program, science, and applications. Remote Sens. Environ. 225, 127–147. https://doi.org/10.1016/j.rse.2019.02.015.
Xiao, X., Zhang, Q., Hollinger, D., Aber, J., Berrien, M., 2005. Modeling gross primary production of an evergreen needleleaf forest using modis and climate data. Ecol. Appl. 15, 954–969. https://doi.org/10.1890/04-0470.
Zhu, Z., Woodcock, C.E., 2012. Object-based cloud and cloud shadow detection in Landsat imagery. Remote Sens. Environ. 118, 83–94. https://doi.org/10.1016/j.rse.2011.10.028.